LONG TERM TRACKING OF HIGH INTENSITY BUNCHED BEAMS WITH COLLISIONALITY

A. Engeda*, Goethe University Frankfurt, Frankfurt am Main, Germany
G. Franchetti, GSI Helmholtz Centre for Heavy Ion Research, Darmstadt, Germany

Abstract

Modeling binary Coulomb collisions directly in particle-in-cell (PIC) simulations is computationally demanding. For long-term studies of intrabeam scattering (IBS), simulations must be both efficient and physically accurate, which requires careful numerical treatment of the statistical representation of the real beam. To address these challenges, a PIC solver with a Monte-Carlo-based Coulomb collision model (PIC–MCC) has been developed within the MICROMAP library written in gfortran for multi passing (MPI/OPENMP) computation. It combines a fully three-dimensional spectral Poisson solver for space–charge computations with established binary Coulomb collision algorithms to model Coulomb scattering (Takizuka and Abe algorithm) [1]. The objective is to obtain reliable predictions of IBS driven influence on the emittance growth and beam lifetime. For validation, MICROMAP also has implemented analytical IBS models such as the Bjorken–Mtingwa (BM) and the Martini formalisms [2–6]. Long-term PIC simulations are compared with analytical predictions to provide a consistent benchmark for assessing the accuracy of the collision models.

INTRODUCTION

Scattering caused by binary elastic interactions between two charged particles through their electromagnetic fields is referred to as a Coulomb collision. Intrabeam scattering (IBS) arises from the cumulative effect of many small-angle Coulomb encounters between particles in high-intensity beams which leads to growth of transverse emittance [2–4]. In kinetic theory, IBS corresponds to collisional relaxation governed by the Fokker–Planck–Landau collision operator [7, 8]. Analytical growth rates widely used in accelerator physics are derived from the formalisms of A. Piwinski [2,3] and Bjorken–Mtingwa [4]. These theories typically assume Gaussian phase-space distributions, smooth focusing approximation, and weak collective perturbations. This framework allows for the simultaneous treatment of collective space–charge forces and stochastic Coulomb scattering within a particle beam. These assumptions limit the applicability of analytical models in strongly nonlinear or non-Gaussian regimes, where PIC simulations provide a more general description.

Comparison of Analytical IBS Model with PIC-MCC

To validate the binary collision model implemented, the numerical results are compared with analytical IBS growth rates obtained from the extended Conte–Martini (CM) model presented in [5, 6] with more advanced analytical models where the non-ultrarelativistic corrections and the effect of vertical dispersion are incorporated [9].
The comparison is performed using identical beam parameters in both approaches in order to establish a consistent benchmark between the particle-based simulation and the theory. The analytical model assumes a Gaussian beam distribution and neglects collective effects such as space–charge.
The IBS growth rates in the analytical model are determined from the evolution of the beam parameters according to

$$\frac{1}{\tau_i} = \frac{1}{\epsilon_d}\frac{d\epsilon_d}{dt}, \quad d \in \{x, y, s\}, \tag{1}$$

where ϵ_d denotes the emittance in the respective plane.
In particle simulation, each particle undergoing a collision is scattered according to the Monte Carlo collision (MCC) model based on the Takizuka–Abe (TA) algorithm [1]. The ion–ion angular collision frequency ν_{ii} provides a measure of the rate of cumulative small-angle Coulomb scattering in the beam frame and is given with

$$\nu_{ii} = \frac{nq^4 \ln\Lambda}{\epsilon_0^2 m_i^2 v_{eff}^3}, \tag{2}$$

where n is the beam density, q the particle charge, m_i the ion mass, v_{eff} effective thermal velocity and $\ln\Lambda$ the Coulomb logarithm. Why this is nessesary to know will be shown in the section of the "Numerical Tests".

MODELING COLLISIONAL PARTICLE TRACKING

The evolution of the particle distribution function $f(\mathbf{x}, \mathbf{v}, t)$, including binary collisions, is described by the Fokker–Planck–Landau equation [7],

$$\frac{\partial f_i}{\partial t} + \mathbf{v}_i \cdot \nabla_x f_i + \frac{q_i}{m_i}\mathbf{E} \cdot \nabla_v f_i = C[f_i, f_j], \tag{3}$$

where $C[f_i, f_j]$ denotes the Landau collision operator describing binary interactions between ions i and j. In its Boltzmann form, the collision operator can be written as

$$C[f_i, f_j] = \int_{\mathbb{R}^3} d\mathbf{v}_j \int_{S^2} d\Omega \left(\frac{d\sigma}{d\Omega}\right) |\mathbf{u}| \left(f_i' f_j' - f_j f_i\right), \tag{4}$$

where $\mathbf{u} = \mathbf{v}_i - \mathbf{v}_j$ is the relative velocity and (f_i', f_j') denote the post-collision distribution functions. The differential scattering cross section for Coulomb interactions is given

* engeda@iap.uni-frankfurt.de

by the Rutherford formula,

$$\frac{d\sigma}{d\Omega} = \frac{(q_i q_j)^2}{16\pi^2 \epsilon_0^2 m_{\mathrm{rel}}^2 u_{\mathrm{rel}}^4}. \tag{5}$$

It is valid in the weakly coupled regime, where the kinetic energy dominates over the potential energy (Γ=U_{pot}/E_{kin} $\ll 1$) and small–angle scattering is the dominant interaction mechanism. The binary collision method of TA is employed [1], see next section. This Monte Carlo scheme reproduces the velocity-space moments of the Fokker–Planck operator while conserving total momentum and kinetic energy.

Takizuka–Abe Binary Collision Model

The Takizuka–Abe model is a grid-based algorithm that provides a stochastic particle realization of the Fokker–Planck–Landau collision operator for small-angle Coulomb scattering. The variance of the deflection angle is chosen such that the resulting momentum exchange reproduces the diffusion described by the Landau collision operator [10–13]. The model is valid in the regime where the collision time $\Delta\tau_{ii}$ determined from the collision frequency ν_{ii} for ion–ion interaction is much smaller than the integration step, ensuring that individual binary interactions remain uncorrelated. This approach therefore provides an efficient and physically consistent method for incorporating Coulomb collisions into particle-in-cell simulations. An efficient particle sorting method for identifying near collision partners is described in [14] where particles are listed belonging to the same mesh-cell. Further with this approach macro-particle within the same spatial cell and the neighboring cells are randomly paired. For these cells, containing N_{cell} particles, the number of collision pairs per timestep is $N_{coll} = \frac{1}{2}N_{\mathrm{cell}}$, where each macro-particle represents a large number of physical particles. Therefore, a single binary interaction statistically represents many physical Coulomb encounters.

Collisional Tracking

For a pair of particles i and j, the relative velocity is

$$\mathbf{u} = \mathbf{v}_i - \mathbf{v}_j, \tag{6}$$

with magnitude $u_{rel} = |\mathbf{u}|$. The mean squared deflection angle over a timestep Δt is obtained from the Landau collision operator,

$$\langle \delta^2 \rangle = \frac{4\pi n q_i^2 q_j^2 \ln\Lambda}{(4\pi\epsilon_0)^2 m_{\mathrm{red}}^2 u_{rel}^3}\Delta t, \tag{7}$$

where δ is a random variable related to θ with $\delta \equiv \tan(\theta/2)$. n is the local particle density, $\log(\Lambda)$ is the Coulomb logarithm and m_{red} the reduced mass. The stochastic variable is sampled as

$$\delta = \sqrt{\langle \delta^2 \rangle}\,\mathcal{N}(0,1), \tag{8}$$

where $\mathcal{N}(0,1)$ denotes a normal distributed random variable with zero mean variance. The scattering angle is then obtained from relation above [1]. The Coulomb logarithm accounts for the range of impact parameters contributing to small-angle scattering and is defined as

$$\log(\Lambda) = \ln\left(\frac{b_{\max}}{b_{\min}}\right). \tag{9}$$

Here $b_{\min}$ corresponds to the classical distance of closest approach, while $b_{\max}$ is determined by the characteristic length scale of the beam, typically chosen as the transverse rms beam size or the Debye screening length when collective effects are present.
In the present study, identical assumptions for $b_{\min}$ and $b_{\max}$ are used in both the PIC simulations and the analytical IBS calculations in order to ensure a consistent comparison. The azimuthal scattering angle is chosen uniformly as

$$\varphi = 2\pi\xi, \tag{10}$$

where ξ is a uniform random number in the interval $[0, 1]$. The relative velocity vector is then rotated according to

$$\mathbf{u}' = R(\theta, \varphi)\mathbf{u}, \tag{11}$$

where $R(\theta, \varphi)$ denotes the rotation operator defined by the polar angle θ and azimuthal angle φ. The post-collision particle velocities are obtained by transforming back to the laboratory frame,

$$\mathbf{v}_i' = \mathbf{v}_i + \frac{\mathbf{u}'}{2}, \quad \mathbf{v}_j' = \mathbf{v}_j - \frac{\mathbf{u}'}{2}. \tag{12}$$

Therefore, both total momentum and kinetic energy are conserved while the correct velocity-space diffusion coefficients are reproduced.

NUMERICAL TESTS

For the benchmark study presented here, space–charge forces are disabled in the PIC solver to enable a direct comparison with analytical IBS models, which neglect space–charge effects. To evaluate the implemented collision model, simulations are performed for a bunched beam propagating through a periodic FODO element that provides transverse focusing. The length of a single FODO channel is 2m. In addition to the baseline simulations, cases marked with an asterisk (*) correspond to runs in which the integration timestep Δt is increased from kick per cell to kick every 50th cell. This allows to assess the sensitivity of the collision model to the condition $\nu_{ii}\Delta t \ll 0.1$, which is required for the validity of the Takizuka–Abe algorithm and met. If this condition is violated, multiple collisions may effectively occur within a single timestep, potentially leading to a wrong estimation of diffusion. The beam consists of a bunch of 10^{11} fully stripped gold ions and is initialized with the parameters listed in Table 1. To analyze the effect of statistical noise due to the number of macro-particles, two simulations with different macrop-article numbers (1×10^4 and 2×10^5) are performed.

The simulations track the evolution of the beam distribution over many FODO periods while computing the transverse rms emittance growth and longitudinal rms momentum

Table 1: Initial simulation parameters.

Parameter	Value	Unit
RMS emittance	1	mm mrad
RMS bunch length	10	mm
RMS $\Delta p/p$	1×10^{-4}	–
Energy per nucleon	10	GeV
Lorentz factor γ_0	11.79	–
Meshgrid, near field [14]	$40 \times 40 \times 40$	–

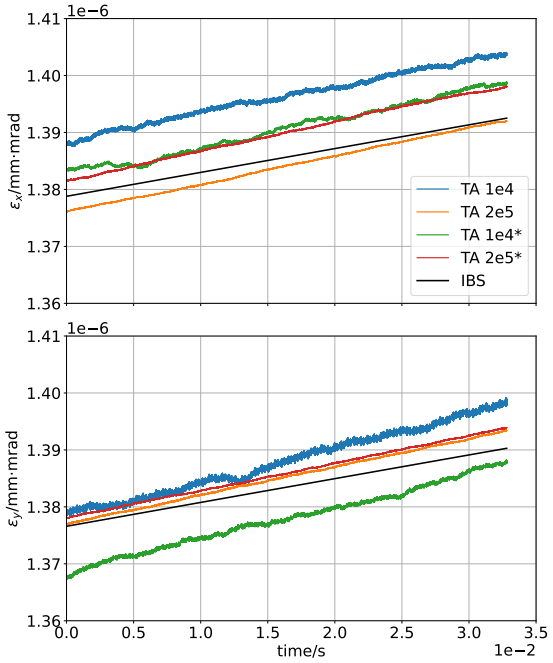

Figure 1: Evolution of the transverse rms emittances, with ϵ_x presents the horizontal emittance and ϵ_y the vertical. The curves labeled with (*) correspond to simulations with an increased timestep Δt.

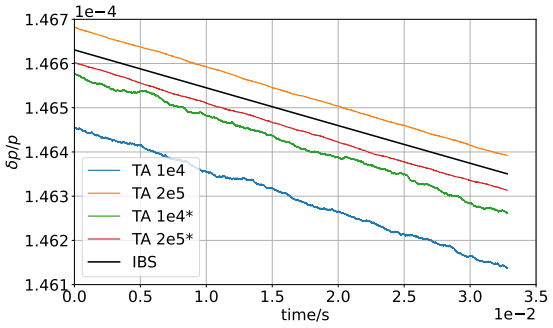

Figure 2: Evolution of the relative momentum spread $\delta p/p$. Increased timestep cases (*) show the sensitivity of the collision model to timestep size.

spread. The obtained growth rates are compared with predictions from the IBS theory.

The results shown in Fig. 1 and Fig. 2 demonstrate that the PIC-MCC simulations reproduce the qualitative behavior of intrabeam scattering as predicted by analytical model. In particular, the transverse emittances exhibit a linear growth, while the longitudinal momentum spread decreases. The decrease in longitudinal momentum spread is consistent with energy redistribution due to IBS, where transverse heating is accompanied by longitudinal cooling.

Table 2: Growth rate for the different models and macro-particle numbers. Cases marked with (*) correspond to the simulation with increased timestep.

Model/ Intensity	Horizontal 10^{-7} [1/s]	Vertical 10^{-7} [1/s]	Longitudinal 10^{-6} [1/s]
TA / 10^4	4.70	6.04	-9.69
TA / 2×10^5	4.94	4.98	-8.87
TA* / 10^4	5.01	5.73	-9.51
TA* / 2×10^5	5.14	4.81	-8.85
Martini Mod.	4.18	4.17	-8.54

A quantitative comparison of the growth rates is provided in Table 2. For the baseline simulations, the transverse growth rates obtained with the Takizuka–Abe model show a faster growth in comparision to the analytic IBS predictions. The influence of the number of macro-particles is clearly visible. Increasing the particle number from 10^4 to 2×10^5 reduces statistical uncertainty and fluctuation and leads to more stable growth rates. The simulations with increased timestep (marked with *) show a marginal deviation from the baseline results which confirmes the condition $\nu_{ii}\Delta t \ll 1$ is met.

DISCUSSION

The comparison between the PIC-MCC simulations and the analytical IBS models shows good agreement in the evolution of the transverse emittances, indicating that the implemented Takizuka–Abe collision model, correctly reproduces the expected collisional diffusion in this scenario. The analytical IBS models rely on assumptions such as Gaussian distributions and smooth focusing, which are satisfied in the numerical simulations. The results demonstrate that the PIC–MCC framework provides a physically consistent description of Coulomb collisions in high–intensity beams. Overall, the agreement between PIC–MCC simulations and analytical IBS models confirms that the implemented collision algorithm provides a consistent description of Coulomb scattering in high-intensity beams for the case presented.

REFERENCES

[1] T. Takizuka and H. Abe, "A binary collision model for plasma simulation with a particle code", *J. Comput. Phys.*, vol. 25, no. 3, pp. 205–219, 1977. doi:10.1016/0021-9991(77)90099-7

[2] A. Piwinski, "Intra-beam-scattering", 1974, doi:10.5170/CERN-1992-001.226, https://cds.cern.ch/record/400720,

[3] A. Piwinski, "Intra-beam scattering", in *Frontiers of Particle Beams*, pp. 297–309, 1988.

[4] J. D. Bjorken and S. K. Mtingwa, "Intrabeam scattering", *Part. Accel.*, vol. 13, pp. 115–143, 1983.

[5] M. Martini, "Intrabeam scattering in the ACOL-AA machines", CERN, Geneva, Switzerland, Rep. CERN-PS-84-9-AA, 1984. https://cds.cern.ch/record/151638

[6] M. Martini, "Intrabeam scattering: anatomy of the theory", *CERN Yellow Rep. School Proc.*, vol. 3, pp. 291–351, 2017. doi:10.23730/CYRSP-2017-003.291

[7] L. D. Landau, "The transport equation in the case of coulomb interactions", *Phys. Z. Sowjetunion*, vol. 10, 1936. doi:10.1016/B978-0-08-010586-4.50029-8

[8] R. Hager, E. S. Yoon, S. Ku, E. F. D'Azevedo, P. H. Worley, and C. S. Chang, "A fully non-linear multi-species fokker–planck–landau collision operator for simulation of fusion plasma", *J. Comput. Phys.*, vol. 315, pp. 644–660, 2016. doi:10.1016/j.jcp.2016.03.064

[9] F. Antoniou and F. Zimmermann, "Revision of intrabeam scattering with non-ultrarelativistic corrections and vertical dispersion for MAD-X", CERN, Geneva, Switzerland, Rep. CERN-ATS-2012-066, 2012. https://cds.cern.ch/record/1445924

[10] Y. Zhao *et al.*, "Modeling of emittance growth due to coulomb collisions in plasma-based accelerators", *Phys. Plasmas*, vol. 27, no. 11, p. 113105, 2020. doi:10.1063/5.0023776

[11] C. Wang, T. Lin, R. Caflisch, B. I. Cohen, and A. M. Dimits, "Particle simulation of coulomb collisions: comparing the methods of takizuka and abe and nanbu", *J. Comput. Phys.*, vol. 227, no. 9, pp. 4308–4329, 2008. doi:10.1016/j.jcp.2007.12.027

[12] B. I. Cohen, A. M. Dimits, and D. J. Strozzi, "A grid-based binary model for coulomb collisions in plasmas", *J. Comput. Phys.*, vol. 234, pp. 33–43, 2013. doi:10.1016/j.jcp.2012.08.046

[13] A. Tanaka, K. Ibano, T. Takizuka, and Y. Ueda, "A coulomb collision model for weighted particle simulations with energy and momentum conservation", *Contrib. Plasma Phys.*, vol. 58, no. 6–8, pp. 451–456, 2018. doi:10.1002/ctpp.201700121

[14] A. Engeda and G. Franchetti, "Macroparticle collisionality in PIC solver", *J. Phys.: Conf. Ser.*, vol. 2687, no. 6, p. 062028, 2024. doi:10.1088/1742-6596/2687/6/062028